Cement and Concrete Research 39 (2009) 433–439

Contents lists available at ScienceDirect

Cement and Concrete Research

journal homepage: http://ees.elsevier.com/CEMCON/default.asp

Early hydration and setting of Portland cement monitored by IR, SEM and Vicat techniques

Rikard Ylmén, Ulf Jäglid, Britt-Marie Steenari, Itai Panas *

Department of Chemistry and Biotechnology, Environmental Inorganic Chemistry, Chalmers University of Technology, S-41296 Gothenburg, Sweden

ARTICLE INFO

Article history:
Received 26 November 2007
Accepted 30 January 2009

Keywords:
Hydration
Calcium-silicate-hydrate (C-S-H)
Spectroscopy
Cement paste
Portland cement

ABSTRACT

Diffuse Reflectance Infrared DR-FTIR spectroscopy is employed to monitor chemical transformations in pastes of Portland limestone cement. To obtain a sufficient time resolution a freeze-dry procedure is used to instantaneously ceasing the hydration process. Rapid re-crystallization of sulphates is observed during the first 15 s, and appears to be complete after ~30 min. After ~60 min, spectroscopic signatures of polymerizing silica start to emerge. A hump at 970–1100 cm^{-1} in conjunction with increasing intensity in the water bending mode region at 1500–1700 cm^{-1} is indicative of the formation of Calcium Silicate Hydrate, C-S-H. Simultaneously with the development of the C-S-H signatures, a dip feature develops at 800–970 cm^{-1}, reflecting the dissolution of Alite, C_3S. Setting times, 180 (initial) and 240 (final) minutes, are determined by the Vicat technique. Combining DR-FTIR, SEM and Vicat measurements it is concluded that the setting is caused by inter-particle coalescence of C-S-H.

1. Introduction

Today, Portland cement is a widely used binder in concrete construction. C_3S (alite) and C_2S (belite) is essential to the build-up of strength in Portland cement. These two calcium-silicate phases are formed above 800 °C, where C_3S is preferentially formed upon elevating the temperature and increasing amount of added burned lime, CaO. C_3S is responsible for short term strength development (days to months) while C_2S displays the better long term strength development performances (~years). The quest for increasingly shorter setting time and early strength has seen the C_3S/C_2S ratio increase in commercial Portland cement. In recent years, the increased attention on environmental aspects of material conversion has influenced research towards possible modifications of Portland cement to better meet the increasing demands for sustainability in the construction sector. This is done by using additives and changing the composition of the cement. Many different experimental techniques have been employed to investigate the effects on material conversion as Portland cement is dissolved and transformed into calcium-silicate-hydrate, C-S-H. For determination of setting times, Vicat measurements are often employed. At later stages in the hydration process, an ultrasonic cement analyser may be used to determine changes in the elastic modulus of the mortar [1,2]. Calorimetry is employed to monitor the heat released upon hydration [3–7], whereas X-ray diffraction [8–13], nuclear magnetic resonance [14–16] and Fourier transform infrared spectroscopy, FTIR, are used to obtain chemical information. Morphological information may be obtained by means of scanning electron microscopy and transmission electron microscopy [11,12,15,17].

Spectroscopic methods are commonly used to study the chemistry of cement hydration. In the present work the hydration of Portland cement has been monitored mainly by means of infrared spectroscopy. In infrared spectroscopy one utilizes that molecules or groups of atoms on large molecules absorbs different wavelengths of infrared light depending on which atoms that constitute the molecule or group, its geometry and its immediate surroundings. It can therefore be used to study both crystalline and amorphous samples. The sample is irradiated with infrared light with a span of different wavelengths. The sample will absorb some of the light at wavelengths that are characteristic to its chemical composition. To see at which wavelengths the sample has absorbed light the intensity at each wavelength is measured with and without sample. IR radiation only penetrates about 1 wavelength into the sample (~10 μm for 1000 cm^{-1}), making it ideal in the study of surface processes.

In previous studies where FTIR was used to study the hydration of cement and its components, the sample was prepared by mixing the cement with KBr and pressing the mixture into pellets [18–21]. The usefulness of Diffuse Reflectance Fourier Transform Infrared Spectroscopy, DR-FTIR, as a tool for studying the hydration of cement has also been demonstrated in previous work [22,23]. A comparison between DR-FTIR and the KBr pellet technique has been done by Delgado et al. [24], who showed that the methods produce similar spectra. The advantage of the KBr technique is that it provides better defined bands than DR-FTIR, but the sample preparation is more labour intensive. The results of the present study suggest that the DR-FTIR technique employed is indeed

* Corresponding author. Tel.: +46 31 7722860; fax: +46 31 7722853.
E-mail address: itai@chalmers.se (I. Panas).

0008-8846/$ – see front matter © 2009 Elsevier Ltd. All rights reserved.
doi:10.1016/j.cemconres.2009.01.017

preferred in that external physico-chemical interference is minimized, i.e. the hydration products are studied in the proper cement matrix with a minimum of sample tampering, and avoiding contact with foreign chemicals. Differential IR light absorption of samples which have been allowed to hydrate for different times is reported here.

Water displays strong absorption in the mid-IR range, which makes it virtually impossible to perform *in situ* studies of cement hydration. A second draw back of *in situ* DR-FTIR for the study of cement hydration is that the surface of the cement paste, while hydrating, may become too flat for the diffuse reflectance technique to be efficiently used. These considerations validate selection of an *ex situ* DR-FTIR approach.

To study very early hydration using an *ex situ* technique, it is imperative that the hydration is stopped instantaneously at a predetermined time. To satisfy this requirement, a freeze-dry technique is adopted in this research. The freezing of the sample with liquid nitrogen ensures that all chemical processes are very much retarded, while the subsequent water evaporation step at low temperature minimizes any thermally induced chemical transformations other than water removal while drying. Indeed, earlier microscopy work [25–27] has shown that freezing is a relatively mild method to stop hydration. The drying will of course affect the structures of some phases. Bound water, like in ettringite, could be partially removed, and morphological properties may change upon removal of water.

The purpose of the present study is to demonstrate the efficiency of the freeze-dry procedure in conjunction with DR-FTIR spectroscopy for studying the complex hydration chemistry of Portland cement. An attempt to correlate relevant spectroscopic signatures to the development of strength in the system is also made. Strength development is monitored here by means of Vicat measurements.

2. Experimental

The Portland cement used was a Portland limestone cement, "byggcement Std PK Skövde CEM II/A-LL 42,5 R", from Cementa AB. An automatic/manual mortar mixer 39-0031 from ELE International was used. The cement was mixed with distilled deionized water that was poured into the mixing bowl before adding the cement. The ratio of water to as received dry cement was 0.4 by weight in both DR-FTIR and Vicat measurements. The cement was carefully added and the paste was mixed at 140 rpm on the mixing blade and 62 rpm on the mixing head. The hydration time was measured from the instant when the cement was added to the water.

2.1. DR-FTIR

The spectrometer used was a Nicolet Magna-IR 560 with an insert cell for diffuse reflectance spectroscopy. The measurement range lies between 400 and 4000 cm^{-1}. The diffuse reflectance technique is utilized, in which the incident beam is allowed to be reflected off the ground sample towards an overhead mirror upon which the diffusely scattered rays are collected and measured in the detector. A more detailed description is given by Fuller and Griffiths [28]. The sample is scanned 64 times with a resolution of 2.0 cm^{-1} and the presented data is an average value. Each sample was prepared and analyzed 3 times and the final spectrum was an average of these 3 measurements to minimize differences due to sample preparation.

The batch size was 200 g of as received dry cement. As the cement hydration was studied from 15 s the cement paste was only mixed for 15 s. However, the chemical development of the cement paste was found to be insensitive of mixing time as long as the cement was completely wetted [29]. Samples were prepared in plastic dishes of 35 mm in diameter. The thickness of the paste in the dishes was ~2–3 mm. Lids were placed over the dishes while they hydrated to prevent water from evaporating. The samples were hydrated between 15 s and 360 min in normal laboratory environment, then frozen by immersion in liquid nitrogen and subsequently placed in the freeze drier overnight. Measurements were made the following day. Before measurement the sample was ground and placed in the sample holder of the DR-FTIR spectrometer. To obtain good reproducibility, great care was taken when grinding the samples and placing them in the sample cup to make the samples as similar as possible.

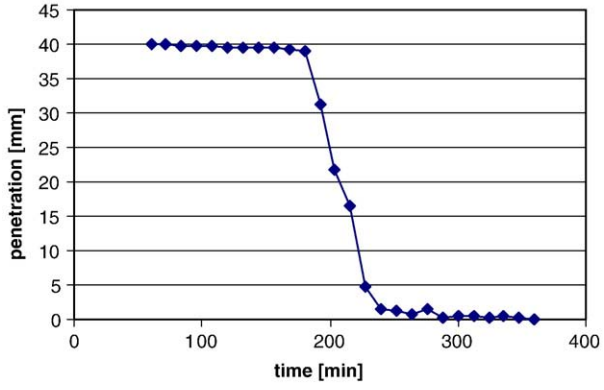

Fig. 1. Vicat measurement showing the depth of penetration of the Vicat needle into the cement as function of time. The height of the mould was 40 mm.

Table 1
Possible assignment to some of the peaks observed in Figs. 2–5.

Wave number [cm^{-1}]	Possible assignment	Reference
656–658	υ_4 of SiO_4	[21,40]
714	υ_4 of CO_3	[22,32,35,37]
847–848	Al–O, Al–OH	[21,35]
877–878	υ_2 of CO_3	[21,22,35,37]
1011–1080	Polymerized silica	[19]
~1100–1200	υ_3 of SO_4	[19,22,31,32]
1200–1202	Syngenite, thenardite	[32–34]
1400–1500	CO_3	[19,21,22,35,37]
1620–1624	υ_2 of water in sulphates	[22,31,33]
1640–1650	υ_2 H_2O	[21,35,36]
1682–1684	υ_2 of water in sulphates	[22,31,33]
1795–1796	$CaCO_3$	Own measurement, [22]
2513–2514	$CaCO_3$	Own measurement, [22]
2875–2879	$CaCO_3$	Own measurement, [22]
2983–2984	$CaCO_3$	Own measurement, [22]
3319–3327	Syngenite, thenardite	[32–34]
3398–3408	υ_3 of H_2O, capillary water	[36]
3457	$\upsilon_1+\upsilon_3$ of H_2O	[21,36]
3554	υ_3 of H_2O in gypsum	[22,31]
3611	Bassanite	[22]
3641–3644	$Ca(OH)_2$	Own measurement, [20,23,24,37]

2.2. Vicat

The batch size was 300 g of as received dry cement and the cement paste was mixed for 2*90 s with a stop in between for 15 s to scrape the paste from the inside walls. The Vicat apparatus used was a Vicatronic automatic recording apparatus E040 and measurements were performed in a 40 mm mould with a calibrated weight of 300 g and a cylindrical needle with flat tip area of 1 mm^2.

2.3. Scanning electron microscopy

The microscope used was a FEI Quanta 200 FEG ESEM operated in secondary electron detection mode with high-vacuum and an acceleration voltage of 2 kV. Some of the freeze-dried samples were pulverized. Since the freeze-dried samples were barely holding together this was easily done with a metal spoon. Some of the powder was placed on carbon tape attached to the sample holder.

Several regions were examined to make sure that the observed structures were representative of the sample.

3. Results

The present study attempts to correlate setting with the evolution of spectral features in DR-FTIR spectra during early hydration of cement. The Vicat setting time measurement for the used Portland cement is displayed in Fig. 1. Initial and final set are seen to occur at 180 min and 240 min respectively. In Section 3.1, the overall time evolution of DR-FTIR absorption intensities is presented. Possible assignments of the different bands are shown in Table 1, and interpreted in Sections 3.1.2–3.1.4.

3.1. Time resolved spectra of hydrating cement

The hydration process was monitored for the first six hours by applying the freeze dry method, grinding of sample and subsequently acquiring the DR-FTIR spectra. The recorded absolute spectra of dry and hydrated cement are displayed in Fig. 2. It shows the spectra of the as received dry cement together with the cement just after it has been mixed (15 s), after 180 min and 360 min of hydration. Weak signatures of hydration can be seen in the 900–1200 cm^{-1} region. To enhance these effects, various difference spectra were constructed. In Fig. 3, the difference spectra employ as received dry cement as reference. Now, the spectroscopic features can be seen significantly clearer and we observe the development and saturation band at 1100–1200 cm^{-1} already after 15 s. This is complemented by a more slowly growing feature at 900–1100 cm^{-1}. Because the bands that developed after 15 s cannot be associated with the actual hardening of cement paste, the 15 s spectrum was taken as reference in Figs. 4 and 5. Fig. 3 supports the overall procedure in that a smooth background is observed in the relevant spectral regions. Having found this, Fig. 5 focuses on the 500–2000 cm^{-1} interval and the spectra for twelve different hydration times are displayed.

3.1.1. Sulphate bands

The sulphates originally present in Portland cement are gypsum ($CaSO_4 \cdot 2H_2O$), hemihydrate (bassanite, $CaSO_4 \cdot 0.5H_2O$) and anhydrite ($CaSO_4$). The latter ones are formed when the gypsum is ground with the cement clinker. The heat makes some of the crystal water in the gypsum to dissociate. When water is added to the cement the sulphates react with the aluminate and ferrite phases of the cement to produce AFt phase. This phase in turn reacts further with the aluminate and ferrite phases to form the AFm phase [30].

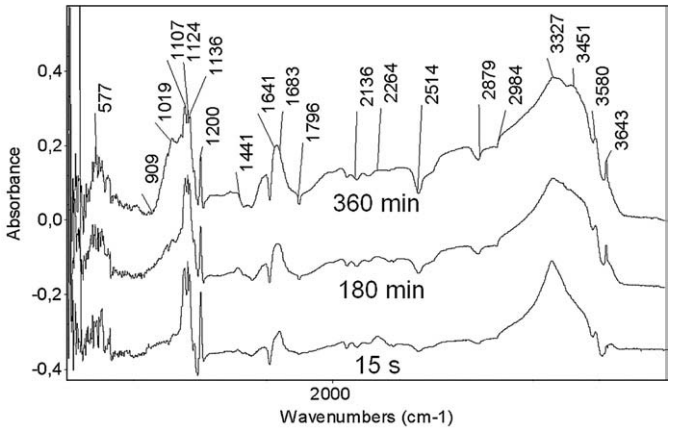

Fig. 3. Difference spectra where the absorbance spectrum of as received dry cement has been subtracted from the absorbance spectra of cement hydrated for 15 s, 180 min and 360 min. The spectra are shown offset for clarity.

Characteristic sulphate absorption bands are generally found in the range 1100–1200 cm^{-1} due to the υ_3 vibration of the SO_4^{2-}-group in sulphates [19,22,31,32]. It is very difficult to interpret this area by studying FTIR-spectra only, since the many forms of sulphates give rise to several peaks here and cause lots of overlaps, but also because the υ_3 vibration of the SiO_4^{2-}-group can absorb in this region, especially when it has polymerized [21]. Therefore no in-depth analysis of it will be done in this work. In the DR-FTIR spectrum of as received dry cement (Fig. 2, bottom spectrum), a broad feature is seen in 1100–1200 cm^{-1} region reflecting mainly amorphous sulphates. Immediately after mixing with water, some sharp absorption bands develop at 1100 cm^{-1}, 1200 cm^{-1} and 3320 cm^{-1}, indicative of very rapid dissolution of sulphates followed by crystallization (Fig. 2, 15 s spectrum). This can also be inferred by considering the 15 s difference spectrum in Fig. 3. This spectrum corresponds to the difference between that acquired after 15 s of hydration, and the spectrum of dry cement. Spectral signatures of sulphate chemistry after 15 s of hydration, corresponding to re-crystallization are obtained. Apparently, crystalline sulphate phases form very early in the hydration process, after which they become inactive spectator phases. The extent to which this holds true can be assessed by replacing the as received dry cement reference spectrum for that of 15 s hydrated cement (Figs. 4 and 5). From Fig. 5 we observe significant changes in the sulphate absorption bands up to 30 min of hydration. Apparently, intermediate phases are formed consistent with the absorption

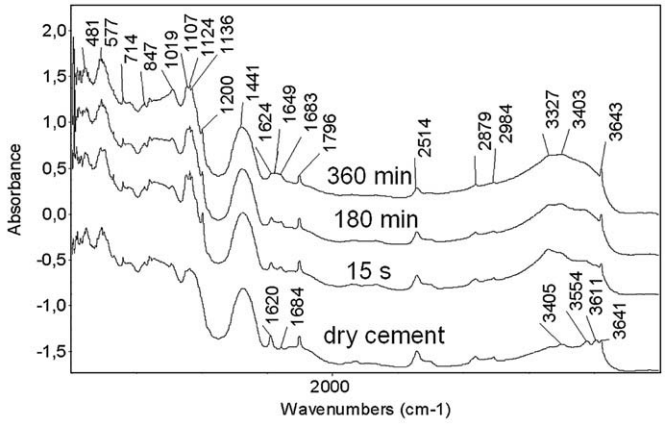

Fig. 2. Absorbance of as received dry cement and cement that has been allowed to hydrate for 15 s, 180 min and 360 min after the cement was added to the water. The spectra are shown offset for clarity.

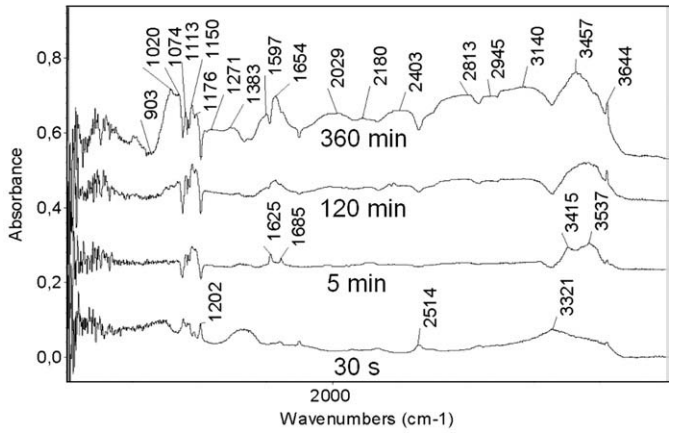

Fig. 4. Difference spectra in the range 400–4000 cm^{-1} where the absorbance spectrum of the freshly mixed cement (15 s) has been subtracted from the absorbance spectra of cement hydrated for 30 s, 5 min, 120 min and 360 min. The spectra are shown offset for clarity.

spectra of syngenite ($K_2Ca(SO_4)_2 \cdot H_2O$) and thenardite (Na_2SO_4) or closely related compounds [32–34]. At any rate, after 60 min, little changes can be seen in the sulphate absorption region of the spectra.

3.1.2. Water associated bands

In the spectrum for as received dry cement there is a peak at 1623 cm^{-1} and a smaller one at 1684 cm^{-1}. These are caused by the bending vibration υ_2 of water in sulphates, mainly gypsum [22,31,33]. The peak at 3554 cm^{-1} is caused by the υ_3 vibration of water in gypsum [22,31] and the peak at 3611 cm^{-1} could be caused by bassanite ($CaSO_4 \cdot 0.5H_2O$). As hydration progresses there is a broad feature forming with its centre at ~1650 cm^{-1}, caused by the bending vibration υ_2 of irregularly bound water [21,35,36]. The consumption of gypsum can be seen as dips in this feature at 1623 cm^{-1} and 1680 cm^{-1} (Figs. 4 and 5). A small increase in gypsum during the first 10 min is implied, and may be due to the transformations of anhydrite and bassanite. The "background" level for wave numbers >1600 cm^{-1} is steadily increasing with increasing hydration times. Since there seems to be no corresponding decrease in any other area, this is probably caused by the incorporation of water. The absorption intensities due to the υ_2 vibration mode of water at ~1650 cm^{-1} and the $\upsilon_1+\upsilon_3$ modes at ~3450 cm^{-1} and results from Mollah et al. and Yu et al. support this observation [21,36].

3.1.3. Silica associated bands

After about 2 h of hydration new spectral intensity shifts are observed from ~900 cm^{-1} towards ~1000–1100 cm^{-1} (see Figs. 3–5), neither associated with sulphates nor water, suggestive of rearrangements in the silica subsystem. These dip-hump features are taken to reflect dissolution of alite and simultaneously the polymerization of silica [21,23,37,38] to form calcium silicate hydrate C-S-H (*vide infra*). In order to focus on the silica chemistry, the 15 s reference spectrum is replaced by that acquired after 30 min (see Fig. 6), i.e. after the sulphate chemistry has stopped. Monotonous growth of the C-S-H associated absorption intensities (970–1100 cm^{-1}) is observed. The dip in the absorption spectrum at 800–970 cm^{-1}, which deepens with time, is due to the dissolution of the C_3S clinker phase [39]. The intensities in the dip (800–970 cm^{-1}) and hump (970–1100 cm^{-1}) regions in Fig. 6 were integrated in an attempt to correlate the clinker dissolution with the silica polymerization. A horizontal line at the intensity at 970 cm^{-1} was used as baseline. The result is plotted in Fig. 7.

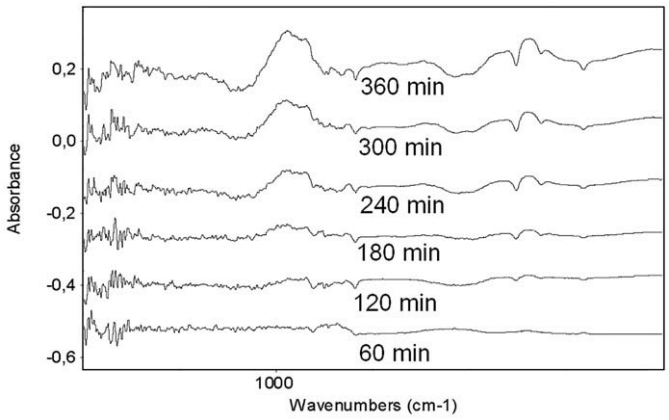

Fig. 6. Difference spectra in the range 500–2000 cm^{-1} where the absorbance spectrum of cement hydrated for 30 min has been subtracted from the absorbance spectra of cement with hydration times from 60–360 min. The spectra are shown offset for clarity.

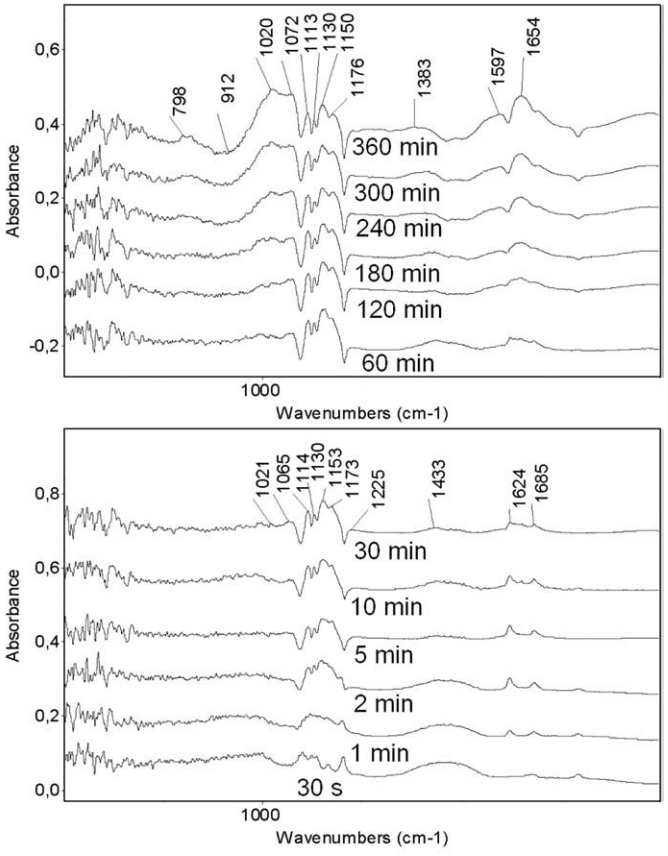

Fig. 5. Difference spectra in the range 500–2000 cm^{-1} where the absorbance spectrum of the freshly mixed cement (15 s) has been subtracted from the absorbance spectra of cement with hydration times from 30 s to 360 min. The spectra are shown offset for clarity.

3.1.4. Hydroxides and carbonates

The peak at 3643 cm^{-1} (see Table 1 and Figs. 2 and 3) corresponds to $Ca(OH)_2$, which is formed as silicate phases in the cement dissolve.

The peaks at 1796 cm^{-1}, 2513 cm^{-1}, 2875 cm^{-1}, 2983 cm^{-1} and the shoulder at 1350–1550 cm^{-1} are due to that portion of calcium carbonate, which is added to the cement by the manufacturer after clinker calcination. The amount of calcium carbonate is seen to decrease as the hydration progresses, i.e. negative absorption bands in the difference spectra of Figs. 3 and 4. This may partly be due to the reaction of calcite with the aluminate to form less crystalline phases such as carboxyaluminates [40,41] or the carbonate ion can substitute for sulphate ions in Aft and AFm phases [13,30]. The peak growing at ~1070 cm^{-1} could be the υ_1 vibration of CO_3-group in the formed carbonates [33,35], but this observation would contradict the overall

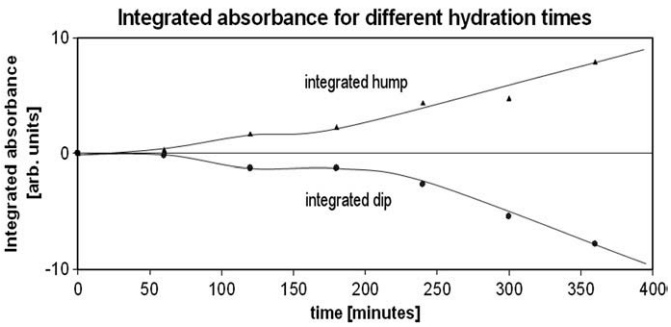

Fig. 7. Integrated value of the absorbance in the intervals 800–970 cm^{-1} (upper dots) and 970–1100 cm^{-1} (lower dots) in Fig. 6 as function of hydration time of the cement. The lines are drawn on free hand to guide the eye and does not represent a mathematical model.

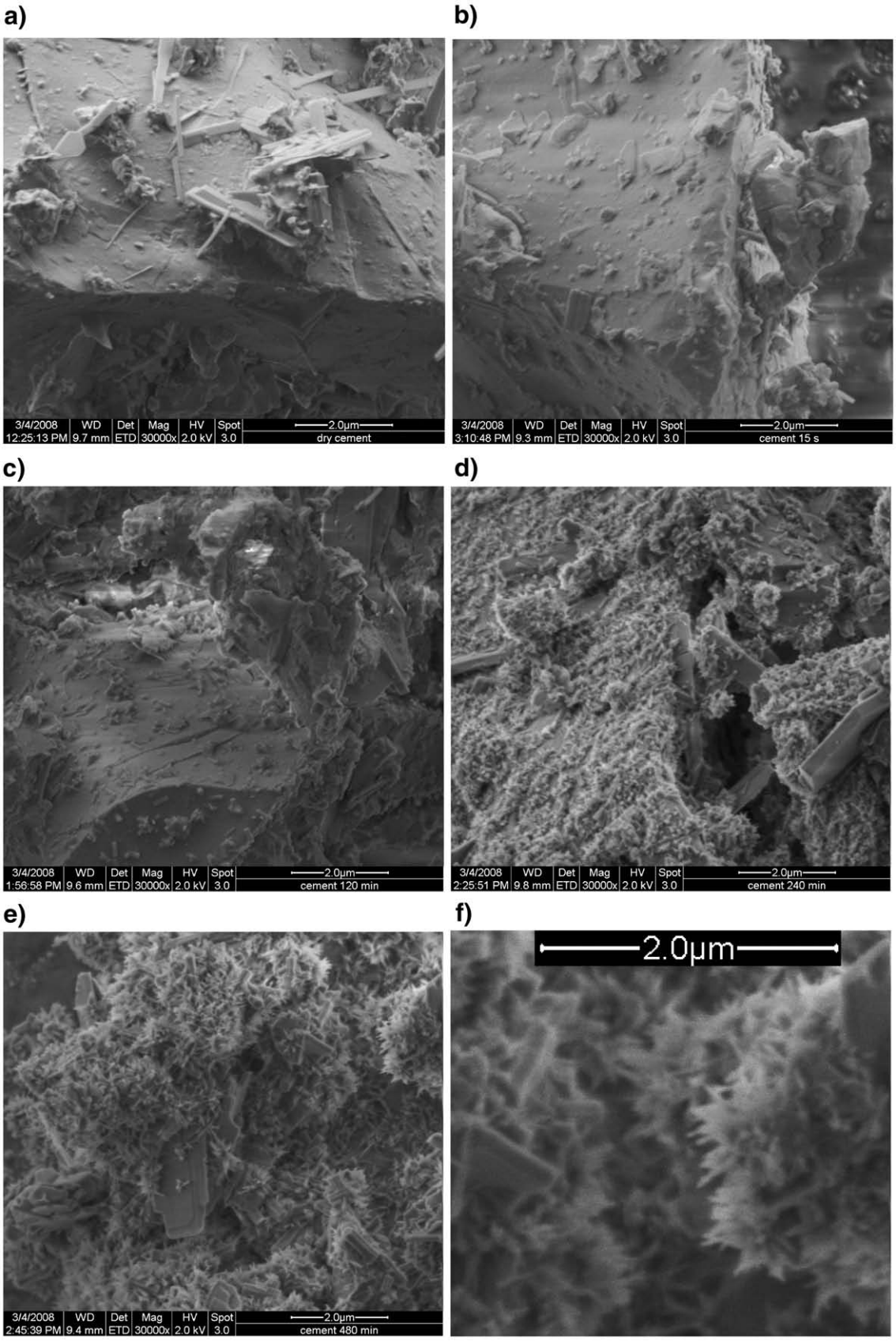

Fig. 8. SEM pictures of cement at different stages of hydration. a) Surface of unhydrated particle. b) Surface of particle hydrated for 15 s. c) Surface of particle hydrated for 120 min. d) Surface of particle hydrated for 240 min. e) Surface of particle hydrated for 480 min. f) Surface of particle hydrated for 480 min at larger magnification.

reduction of carbonate absorption intensities with time. A more plausible candidate for this absorption band is the stretching vibration of Si–O, which is also found in jennite ($Ca_8(Si_6O_{18}H_2)(OH)_8Ca\cdot 6H_2O$) [37,38].

3.2. SEM

SEM pictures of cement grains at different stages of hydration are displayed in Fig. 8. The surfaces of the unhydrated particles are bare, with debris lying on top (Fig. 8a). After 15 s and 120 min of hydration (Fig. 8b, c) the surfaces of the cement particles are still found to be bare, but lumps and platelets have formed in addition to the debris present already on the unhydrated particles. Fig. 8d shows cement after 240 min of hydration. Now a carpet is covering the cement particles. The carpet has grown even more after 480 min of hydration and is seen to consist of needle-like protruding structures (Fig. 8e, f).

4. Discussion

A longstanding issue concerns the roles of various phases during early hardening of Portland cement. In particular the roles of sulphates, added to the Portland cement as anhydrous ($CaSO_4$), hemihydrate ($CaSO_4\cdot 0.5H_2O$), and gypsum ($CaSO_4\cdot 2H_2O$) have been much discussed in this context. Indeed, the general consensus is that the dissolution and re-crystallization of the various sulphate containing phases is completed well before the setting occurs [42,43]. Yet, due to the complexity and instability of the early cement chemistry, the sulphates, besides their well known function as water absorbents, have been empirically found to affect the morphology of the hydrating paste both by providing a background ionic strength and by forming intermediate phases, which suppress “flash setting”. In the present study, results show that the sulphate related DR-FTIR absorption bands display large changes in the 1100–1200 cm^{-1} interval but that this occurs mainly during the first 10 min of hydration, during which the development of sharp bands imply the formation of crystalline phases. The appearing platelets and hexagonal crystals seen with SEM are possibly associated with these phases. After 30 min, the interconversion of sulphate phases has apparently stopped. The sulphates formed are most probably ettringite or monosulphate, as earlier studies on cement hydration have shown that these sulphates are formed during the first minutes of hydration [11,43,44]. In this study of the evolution of the C-S-H absorption bands, the 30 min spectrum was chosen as reference. The degree to which the sulphate chemistry is completed at this time can be appreciated by studying 1100–1200 cm^{-1} region in Fig. 6, keeping in mind that C-S-H also displays absorption bands in this interval.

By DR-FTIR spectroscopy, detectable amounts of polymerized silica are formed after approximately 1 h of hydration, as seen in Fig. 6 in the 900–1100 cm^{-1} interval. It is gratifying to note how well the integrated intensities at 800–970 cm^{-1} as function of time (Fig. 7) correlate with the quantitative X-ray diffraction study on C_3S hydration by Taylor et al. [45], who interpreted their results to imply C-S-H formation. The fact that the growth of the hump feature at 970–1100 cm^{-1} follows the C_3S dissolution process implies that the signature of polymeric silica indeed corresponds to C-S-H formation. It can be noted how the formation of polymerized silica (970–1100 cm^{-1}) is correlated in time with an increased incorporation of water in the structure as seen in the absorption interval at 1500–1700 cm^{-1}. This supports further that calcium silica hydrate C-S-H is a major product formed upon early Portland cement hydration, as C-S-H consists of polymerized silica and calcium ions with water incorporated.

It becomes interesting to attempt to correlate the materials conversion observed with DR-FTIR with morphological changes as seen with SEM. The acceleration phase of C-S-H formation starts somewhere between 120 and 180 min (Figs. 6 and 7). Simultaneously a growth of a needle-like phase is developed on the cement particles (Fig. 8). This phase has been attributed to C-S-H in previous studies of alite, C_3S, where no other phase than C-S-H and portlandite ($Ca(OH)_2$) is formed [25,46]. It is seen in Fig. 1 that the setting starts after 180 min, and that it is completed after 240 min. Since the conversion of the sulphates occurs during the first 30 min, the possibility that the needle-like phase is due to sulphates is ruled out. However, the acceleration phase of C-S-H formation (*vide supra*) occurs on the same time scale as the formation of the needle-like phase seen by SEM as well as that of the setting process. An identification of C-S-H as the phase responsible for the setting of the Portland cement is thus arrived at. Support is produced to the claim that C-S-H is responsible for the initial development of strength in Portland cement pastes. Also, it is suggested that C-S-H is formed continuously during hydration and in particular so prior to the setting. This implies that the actual setting is due to coalescence of clinker grains and that it is associated with the formation of sufficient amounts of C-S-H, to increase friction and bridge the inter-grain distances.

The present findings are consistent with those of Chen and Odler [43], who reach the conclusion that setting in ordinary Portland cement is mainly due to the formation of C-S-H as long as the ratio between sulphates and $C_3A + C_4AF$ is balanced, else “false setting” results due to the formation of ettringite or monosulphate.

5. Conclusions

Cement is a complex material, and its hydration possibly provides additional complexity. Indeed, as yet no single method exists which completely determines all chemical reactions taking place in a cement structure from the mixing and onward. Therefore several complementary techniques must be used.

In the present study, signatures of early setting of an untampered limestone Portland cement were extracted by correlating DR-FTIR, SEM, and Vicat measurements. The objective of this paper was to demonstrate how diffuse reflectance Fourier transform infrared spectroscopy in combination with freeze-drying may add a piece of the puzzle regarding material conversion during the very early stages of cement hydration, down to fractions of a minute. Whereas setting of each unique cement must be addressed separately, a method to monitor the material conversions during early hydration has been presented.

Summarizing:

- the time evolution of the sulphate chemistry displays very rapid crystallization followed by a slow recrystallization phase, which is completed within approximately 30 min;
- the appearance of a broad absorption hump at 970–1100 cm^{-1} after 60 min of hydration is due to polymeric silica. It is correlated with the development of water bending vibration bands (1500–1700 cm^{-1}). This implies the formation of calcium silicate hydrate, C-S-H;
- time dependent changes in morphology due to the hydration process, as monitored with SEM, were found to correlate with the DR-FTIR signatures of C-S-H formation,
- the growth of a dip feature in the spectra at 800–970 cm^{-1}, identified as the dissolution of C_3S Alite, correlates with the formation of C-S-H.

Vicat setting begins after 180 min and is completed after 240 min. This occurs well after the sulphate reactions have stopped. However, the C-S-H formation in the acceleration phase of C_3S dissolution, displays the same time dependence as that of the setting process. The observations support the understanding of setting in terms of coalescing C-S-H coated Portland cement particles.

Acknowledgements

The support from the Knowledge foundation (KK stiftelsen), the Swedish Research Council, and Eka Chemicals Inc., Bohus is gratefully acknowledged, as well as valuable discussions with Inger Jansson.

References

[1] C. Ljungkrantz, G. Möller, N. Petersons (Eds.), Betonghandbok material, second ed., AB Svensk Byggtjänst, 1994.
[2] V.M. Malhotra, N.J. Carino (Eds.), Handbook on Nondestructive Testing of Concrete, second ed., CRC Press, 2004.
[3] M.A. Smith, J.D. Matthews, Conduction calorimetric studies of the effect of sulphate on the hydration reactions of Portland cement, Cement and Concrete Research 4 (1974) 45–55.
[4] M. Kaminski, W. Zielenkiewicz, The heats of hydration of cement constituents, Cement and Concrete Research 12 (1982) 549–558.
[5] F. Lagier, K.E. Kurtis, Influence of Portland cement composition on early age reactions with metakaolin, Cement and Concrete Research 37 (2007) 1411–1417.
[6] V. Rahhal, et al., Calorimetry of Portland cement with silica fume and gypsum additions, Journal of Thermal Analysis and Calorimetry 87 (2) (2007) 331–336.
[7] J.-C. Wang, P.-Y. Yan, Influence of initial casting temperature and dosage of fly ash on hydration heat evolution of concrete under adiabatic condition, Journal of Thermal Analysis and Calorimetry 85 (3) (2006) 755–760.
[8] K.L. Scrivener, et al., Quantitative study of Portland cement hydration by X-ray diffraction/Rietveld analysis and independent methods, Cement and Concrete Research 34 (2004) 1541–1547.
[9] A.N. Christensen, et al., Real time study of cement and clinker phases hydration, Dalton Transactions (8) (2003) 1529–1536.
[10] N.A. Voglis, G.T. Kakali, S.G. Tsivilis, Identification of composite cement hydration products by means of X-ray diffraction, Microchimica Acta 136 (2001).
[11] P. Gu, J.J. Beaudoin, A conduction calorimetric study of early hydration of ordinary Portland cement/high alumina cement pastes, Journal of Materials Science 32 (1997) 3875–3881.
[12] E.T. Stepkowska, et al., Study of hydration of two cements of different strengths, Journal of Thermal Analysis and Calorimetry 69 (2002) 187–204.
[13] H.-J. Kuzel, Initial hydration reactions and mechanisms of delayed-ettringite formation in Portland cements, Cement and Concrete Composites 18 (1996) 195–203.
[14] K. Johansson, et al., Kinetics of the hydration reactions in the cement paste with mechanochemically modified cement ^{29}Si magic-angle-spinning NMR study, Cement and Concrete Research 29 (1999) 1575–1581.
[15] I.G. Richardson, The nature of the hydration products in hardened cement pastes, Cement and Concrete Composites 22 (2000) 97–113.
[16] J. Hjorth, J. Skibsted, H.J. Jakobsen, ^{29}Si MAS NMR studies of Portland cement components and effects of microsilica on the hydration reaction, Cement and Concrete Research 18 (1988) 789–798.
[17] K.L. Scrivener, Backscattered electron imaging of cementitious microstructures: understanding and quantification, Cement and Concrete Composites 26 (2004) 935–945.
[18] T. Liang, Y. Nanru, Hydration products of calcium aluminoferrite in the presence of gypsum, Cement and Concrete Research 24 (1994) 150–158.
[19] M.Y.A. Mollah, et al., A Fourier transform infrared spectroscopic investigation of the early hydration of Portland cement and the influence of sodium lignosulfonate, Cement and Concrete Research 30 (2000) 267–273.
[20] D.A. Silva, H.R. Roman, P.J.P. Gleize, Evidences of chemical interaction between EVA and hydrating Portland cement, Cement and Concrete Research 32 (2002) 1383–1390.
[21] M.Y.A. Mollah, M. Kesmez, D.L. Cocke, An X-ray diffraction (XRD) and Fourier transform infrared spectroscopic (FT-IR) investigation of the long-term effect on the solidification/stabilization (S/S) of arsenic(V) in Portland cement type-V, Science of the Total Environment (325) (2003) 255–262.
[22] T.L. Hughes, et al., Determining cement composition by Fourier transform infrared spectroscopy, Advanced Cement Based Materials 2 (1995) 91–104.
[23] J. Björnström, Influence of nano-silica and organic admixtures on cement hydration — a mechanistic investigation, Department of Chemistry, Göteborg University, Gothenburg, 2005.
[24] A.H. Delgado, R.M. Paroli, J.J. Beaudoin, Comparison of IR techniques for the characterization of construction cement minerals and hydrated products, Applied Spectroscopy 50 (8) (1996) 970–976.
[25] K.O. Kjellsen, H. Justnes, Revisiting the microstructure of hydrated tricalcium silicate — a comparison to Portland cement, Cement and Concrete Composites 26 (2004) 947–956.
[26] M. Collepardi, B. Marchese, Morphology and surface properties of hydrated tricalcium silicate pastes, Cement and Concrete Research 2 (1972) 57–65.
[27] S. Chandra, B. Hedberg, L. Berntsson, Freezing as a method of study of early cement paste hydration, Cement and Concrete Research 10 (1980) 467–469.
[28] M.P. Fuller, P.R. Griffiths, Diffuse reflectance measurements by infrared Fourier transform spectrometry, Analytical Chemistry 50 (13) (1978) 1907–1910.
[29] R. Ylmén, et al., DR-FTIR method for the study of early hydration of cement, SCC 2008: Challenges and Barriers to Application, Chicago Marriott O'Hare, West Higgins Road, Chicago IL 60631, 2008.
[30] H.F.W. Taylor, Hydrated aluminate, ferrite and sulphate phases, Cement Chemistry, Academic Press, London, 1992, pp. 167–198.
[31] S.N. Ghosh, S.K. Handoo, Infrared and Raman spectral studies in cement and concrete, Cement and Concrete Research 10 (1980) 771–778.
[32] J.T. Kloprogge, et al., Vibrational spectroscopic study of syngenite formed during the treatment of liquid manure with sulphuric acid, Vibrational Spectroscopy 28 (2002) 209–221.
[33] T. Vazquez-Moreno, M.T. Blanco-Varela, Table of infrared frequencies and absorption spectra of compound related to cement chemistry, Materiales de Construccion (182) (1981) 31–48.
[34] S. Martinez-Ramirez, Influence of SO_2 deposition on cement mortar hydration, Cement and Concrete Research 29 (1999) 107–111.
[35] M.A. Trezza, A.E. Lavat, Analysis of the system $3CaO \cdot Al_2O_3$–$CaSO_4 \cdot 2H_2O$–$CaCO_3$–H_2O by FT-IR spectroscopy, Cement and Concrete Research 31 (2001) 869–872.
[36] T. Richard, et al., Diffuse reflectance infrared Fourier transform spectroscopy as a tool to characterise water in adsorption/confinement situations, Journal of Colloid and Interface Science 304 (2006) 125–136.
[37] P. Yu, et al., Structure of calcium silicate hydrate (C-S-H): near-, mid-, and far-infrared spectroscopy, Journal of American Ceramic Society 82 (3) (1999) 742–748.
[38] E.T. Stepkowska, et al., Hydration products in two aged cement pastes, Journal of Thermal Analysis and Calorimetry 82 (2005) 731–739.
[39] J. Bjornstrom, et al., Accelerating effects of colloidal nano-silica for beneficial calcium-silicate-hydrate formation in cement, Chemical Physics Letters 392 (1–3) (2004) 242–248.
[40] J. Péra, S. Husson, B. Guilhot, Influence of finely ground limestone on cement hydration, Cement and Concrete Composites 21 (1999) 99–105.
[41] T. Matschei, B. Lothenbach, F.P. Glasser, The role of calcium carbonate in cement hydration, Cement and Concrete Research 37 (2007) 551–558.
[42] H.F.W. Taylor, Actions of calcium sulphate and of alkalis, Cement Chemistry, Academic Press, London, 1992, pp. 231–234.
[43] Y. Chen, I. Odler, On the origin of Portland cement setting, Cement and Concrete Research 22 (1992) 1130–1140.
[44] M. Merlini, et al., The early hydration and the set of Portland cements: in situ X-ray powder diffraction studies, Powder Diffraction 22 (3) (2007) 201–208.
[45] H.F.W. Taylor, et al., The hydration of tricalcium silicate, Materiaux et Constructions 17 (102) (1984) 457–458.
[46] K.O. Kjellsen, B. Lagerblad, Microstructure of tricalcium silicate and Portland cement systems at middle periods of hydration-development of Hadley grains, Cement and Concrete Research 37 (1) (2007) 13–20.